HAL open science

Stability of Leap-Frog Constant-Coefficients Semi-Implicit Schemes for the Fully Elastic System of Euler Equations. Case with Orography.

Pierre Bénard, Jan Masek, Petra Smolikova

▶ **To cite this version:**

Pierre Bénard, Jan Masek, Petra Smolikova. Stability of Leap-Frog Constant-Coefficients Semi-Implicit Schemes for the Fully Elastic System of Euler Equations. Case with Orography.. 2004. hal-00003241

HAL Id: hal-00003241

https://hal.science/hal-00003241v1

Preprint submitted on 9 Nov 2004

HAL is a multi-disciplinary open access archive for the deposit and dissemination of scientific research documents, whether they are published or not. The documents may come from teaching and research institutions in France or abroad, or from public or private research centers.

L'archive ouverte pluridisciplinaire **HAL**, est destinée au dépôt et à la diffusion de documents scientifiques de niveau recherche, publiés ou non, émanant des établissements d'enseignement et de recherche français ou étrangers, des laboratoires publics ou privés.

Stability of Leap-Frog Constant-Coefficients Semi-Implicit Schemes for the Fully Elastic System of Euler Equations. Case with Orography.

P. Bénard*, J. Mašek+, P. Smolíková†

* *Centre National de Recherches Météorologiques, Météo-France, Toulouse, France*

+ *Slovak Hydro-Meteorological Institute, Bratislava, Slovakia*

† *Czech Hydro-Meteorological Institute, Prague, Czech Republic*

23 June 2004

Corresponding address:

Pierre Bénard

CNRM/GMAP

42, Avenue G. Coriolis

F-31057 TOULOUSE CEDEX

FRANCE

Telephone: +33 (0)5 61 07 84 63

Fax: +33 (0)5 61 07 84 53

e-mail: pierre.benard@meteo.fr

ABSTRACT

The stability of constant-coefficients semi-implicit schemes for the hydrostatic primitive equations and the fully elastic Euler equations in presence of explicitly treated thermal residuals has been theoretically examined in the earlier literature, but only for the case of a flat terrain. This paper extends these analyses to the case where an orography is present, in the shape of a uniform slope.

It is shown, with mass-based coordinates, that for the Euler equations, the presence of a slope reduces furthermore the set of the prognostic variables which can be used in the vertical momentum equation to maintain the robustness of the scheme, compared to the case of a flat terrain. The situation appears to be similar for systems cast in mass-based and height-based vertical coordinates.

Still for mass-based vertical coordinates, an optimal prognostic variable is proposed, and shown to result in a robustness similar to the one observed for the hydrostatic primitive equations system.

The prognostic variables which lead to robust semi-implicit schemes share the property of having cumbersome evolution equations, and an alternative time-treatment of some terms is then required to keep the evolution equation reasonably simple. This treatment is shown not to modify substantially the stability of the time-scheme.

This study finally indicates that with a pertinent choice for the prognostic variables, mass-based vertical coordinates are equally suitable as height-based coordinates for efficiently solving the compressible Euler equations system.

1 Introduction

The semi-implicit (SI) technique was introduced in meteorology by Robert et al. (1972), in order to increase the numerical efficiency with respect to explicit schemes, by allowing larger time-steps. SI schemes are based on an arbitrary separation of the evolution terms between linear contributions, treated implicitly, and non-linear (NL) residuals, treated explicitly.

As discussed in Bénard et al., 2004 (BLSV04 hereafter), several classes of SI schemes can be defined. In order to alleviate the problems linked to NL residuals, SI schemes for which the linear terms have non horizontally-homogeneous coefficients (Thomas et al. 1998), or even non-constant coefficients (Skamarock et al., 1997) can be designed. This latter type of schemes is not examined here since the focus of the present paper is exclusively restricted to the so-called class of "constant-coefficients" SI schemes, that is, to SI schemes in which all the implicit linear terms have their coefficients constant in time and horizontally homogeneous. For this class of SI schemes, the relatively large magnitude of NL residuals can result in instabilities, especially for long time-step. Note however that the stability can then be restored through an iteration of the scheme, as shown in Bénard, 2003 (B03 hereafter).

A theoretical framework for studying analytically the stability of these constant-coefficients SI schemes in presence of thermal NL residuals and in simplified contexts has been proposed by Simmons et al. (1978), Côté et al. (1983), and Simmons and Temperton (1997) for the hydrostatic primitive equation (HPE) system, and extended to the fully elastic Euler equation (EE) system by B03. A more detailed review on the history of these stability analyses for SI schemes can be found in this latter paper. Using the same theoretical framework as in B03, a large sensitivity of the three-time levels (3-TL)

SI scheme stability to the choice of the prognostic variables was demonstrated for the EE system in BLVS04. In particular, the choice of the two new prognostic variables appearing in the EE system due to the relaxation of the hydrostatic hypothesis was shown to have a dramatic impact on the stability. In the case of a general mass-based coordinate η (e.g. Laprise, 1992), an optimal set for these two variables was proposed as follows:

$$\mathcal{P} = \frac{p-\pi}{\pi} \tag{1}$$

$$\mathsf{d} = -\frac{p}{mRT}\frac{\partial w}{\partial \eta} \tag{2}$$

where T is the temperature, w the vertical velocity, p the true pressure, π the hydrostatic-pressure, and $m = (\partial\pi/\partial\eta)$ (in all this paper, see Appendix A for the definition of symbols which are not defined in the text).

Finally, Bénard (2004) showed that an intrinsic instability of the two-time levels SI scheme for the EE system could be eliminated by choosing a slightly modified SI linear reference system, which then can no longer be defined as the tangent-linear operator of the complete system around an existing reference state.

A common point to all the abovementionned studies was to neglect the orography as a source of nonlinear terms, and to focus mainly on the instability induced by the thermal nonlinear residuals (as shown in BLVS04, the nonlinear terms induced by the pressure field can be eliminated in mass-based coordinates by using appropriate coordinates, column-integrated mass variables, and pressure variables). Conversely, in the case where all NL thermal residuals are neglected, Ikawa (1988) showed that explicitly treated orographic terms could make the evolution of compressible systems in height-based coordinates unstable for the particular class of prognostic variables and SI schemes that he examined. It can therefore be suspected that a combination of explicitly treated thermal residuals and

orographic terms could result in new instabilities. In this case, for mass-based coordinate systems, there is no proof that the choice (1)–(2) proposed above is still the most relevant.

This latter statement was confirmed experimentally, by showing that this choice actually led to instability when an orography was introduced in the two-dimensional (vertical plane) version of the cooperative model "Aladin-NH", described in Bubnová *et al.*, 1995, (hereafter BHBG95). The instability could be reproduced even for very simple flows, including initially balanced resting isothermal flows over an isolated mountain.

This experimental fact prompted us to study more in detail the behaviour of the 3-TL SI EE system from the theoretical point of view in presence of orography, in order to investigate the nature of the associated instability and to seek possible remedies. The results of this study are reported in this paper.

The stability analyses presented here are thus valid for the Aladin-NH model (BHBG95) as well as for numerical models that would be based on the same principles (mass-based coordinates, similar linear SI separation, etc).

In section 2, we will define an academic (simplified) framework which allows algebraically tractable stability analyses for the 3-TL SI EE space-continuous system in presence of a simple orography which consists in a "uniform slope mountain"; then the stability of the previously proposed choice (1)–(2) will be examined in section 3. In section 4, an alternative variable $\mathbf{d}$ will be proposed, and shown to result in a better stability in presence of orography. In section 5, a numerical assessment of the validity of the theoretical results will be presented. In sections 6 and 7 some comments concerning the HPE system and an alternative time-treatment of the vertical momentum equation will be developed, and the general conclusion will be presented in section 8.

2 Theoretical framework for analyses

The theoretical framework used for the analyses in this paper is basically the same as in BLVS04, except that an orography is introduced: the EE system is thus cast in the pure unstretched terrain-following hydrostatic-pressure-based $\sigma = (\pi/\pi_s)$ coordinate and the flow is assumed to be dry, adiabatic and inviscid, in a non-rotating atmosphere and a Cartesian framework.

The general set of equations (3)-(9) of BLVS04 is thus still valid, even in presence of orography, and will be used here as a starting point.

The general method for the analyses is also similar to B03 and BLVS04: an "actual" steady basic-state $\overline{\mathcal{X}}$ and a SI-reference state $\mathcal{X}^*$ are chosen, and the analysis is performed for small perturbations around $\overline{\mathcal{X}}$ (see B03 for deeper explanations and notations). Both $\overline{\mathcal{X}}$ and $\mathcal{X}^*$ are assumed isothermal, resting and hydrostatically-balanced. The perturbations around $\overline{\mathcal{X}}$ are assumed to remain small, hence the source terms of the system can be linearized around $\overline{\mathcal{X}}$, and symbolically noted $\overline{\mathcal{L}}$. Similarly, the source terms of the linear reference system associated to the SI scheme are noted $\mathcal{L}^*$. The SI scheme is then implemented according to Eq. (12) of BLVS04, and the residual $(\overline{\mathcal{L}} - \mathcal{L}^*)$ is treated explicitely. The domain is taken as a two-dimensional vertical plane along the x direction. The temperature of the basic actual state $\overline{T}$ deviates from the one of the SI-reference state T^*, thus generating explicitly treated thermal residuals.

As outlined above, the major difference between the framework used in BLVS04 and the present one is that a uniform slope s is now assumed for the surface height z_s of the bottom boundary:

$$z_s(x) = s\,x, \tag{3}$$

hence the surface geopotential is given by $\phi_s(x) = gsx$. Since the domain is assumed unbounded in the x direction in order to later allow simpler normal mode analyses, some care must be taken to assess the physical relevance of this framework.

The column-integrated mass variations are described through the prognostic variable $q = \ln(\pi_s)$. The stationarity of $\overline{\mathcal{X}}$ for the complete system imposes the pressure-gradient force to vanish in the horizontal momentum equation. Hence (using the above assumptions):

$$R\overline{T}\nabla\overline{q} + \nabla\phi_s = 0 \tag{4}$$

or:

$$\nabla\overline{q} = -\frac{gs}{R\overline{T}} \tag{5}$$

where $\overline{q}(x)$ is the q field in the actual state $\overline{\mathcal{X}}$ and ∇ is the $(\partial/\partial x)$ operator along constant σ surfaces. Under all mentionned assumptions, it can be checked easily that $\overline{\mathcal{X}}$ is then a stationary state for the complete system (3)–(9) of BLSV04, and consequently for the linearized system associated to $\overline{\mathcal{L}}$ as well.

It appears that both fields ϕ_s and $\overline{q}$ are unbounded when x becomes unbounded. However, this mathematical feature does not induce any particular problem from the physical point of view, since only spatial or temporal variations of these fields appear in the equations. In other words, even if the height of the orography is unbounded along x, all orographic source terms always remain bounded since the slope s is a finite number. From the physical point of view, the proposed framework is thus perfectly relevant for describing the flow over a slanted unbounded orography.

As outlined in B03, due to the elimination of upper and lower boundary conditions which will be performed in all these analyses, a more "local" point of view can be adopted

and the framework can then be considered as relevant also for describing the evolution of small-scale perturbations inside a limited region of the atmosphere when the larger scale environment is given by $\overline{\mathcal{X}}$. Using this local point of view, the slope s must therefore be understood as the mean slope of the orography at a scale much larger than the scale of the perturbations considered in the analysis. In this paper, we will examine atmospheric perturbations at the kilometric horizontal scale, consistently with future targets for NWP applications, hence, the slopes retained in the analyses will be consistent with terrestrial slopes at an horizontal scale of 50-100 km, that is, $s \in [-0.05, +0.05]$. For smaller (i.e. hectometric) perturbation scales, steeper slopes would have to be considered.

The small perturbation $\widetilde{\mathcal{X}}$ around the $\overline{\mathcal{X}}$ state is defined by:

$$\widetilde{T} = T - \overline{T} \tag{6}$$

$$\widetilde{q} = q - \overline{q}. \tag{7}$$

Since the other prognostic variables have a zero reference-value, the tilde symbol is omitted for them. For the specification of q in the $\mathcal{X}^*$ state, we follow the approach usually adopted in practical NWP applications, that is, $q^* = \ln(\pi_{00})$, where π_{00} is an arbitrary constant. The complete set of equations is then linearized around this q^* value, assuming no orography.

3 Stability analysis with the $\{\mathcal{P}, \mathsf{d}\}$ set of variables

In this section the stability of the 3-TL SI EE system is examined for the set of variables $\{\mathcal{P}, \mathsf{d}\}$ which was proposed in Eqs. (22) and (65) of BLVS04 for eliminating the problems linked with a discrepancy between $\overline{T}$ and T^* in the case of flat terrain. The linearization of the system is performed in the same way as in BLVS04, but now retaining all linear

terms involving s through $\nabla\phi_s$ or $\nabla\overline{q}$. The linearized expression of the three-dimensional divergence D_3 is:

$$D_3 = D + \mathsf{d} + \frac{gs}{R\overline{T}}\tilde{\partial}u \tag{8}$$

where u is the horizontal wind component, $D = \nabla u$, and $\tilde{\partial} = \sigma(\partial/\partial\sigma)$. Additionally, the expression of $(\dot{\pi}/\pi)$ is required for the equation of $\mathcal{P}$ since:

$$\frac{d\mathcal{P}}{dt} = (1+\mathcal{P})\left(\frac{\dot{p}}{p} - \frac{\dot{\pi}}{\pi}\right) \tag{9}$$

The linearized version of $(\dot{\pi}/\pi)$ writes:

$$\left(\frac{\dot{\pi}}{\pi}\right) = -\mathcal{S}D - \frac{gs}{R\overline{T}}(\mathcal{I}-\mathcal{S})u \tag{10}$$

and the linearized $\overline{\mathcal{L}}$ system with orography becomes:

$$\begin{aligned}
\frac{\partial D}{\partial t} &= -R\overline{T}\nabla\nabla'\left[\mathcal{G}\frac{\widetilde{T}}{\overline{T}} - (\mathcal{G}-\mathcal{I})\mathcal{P}\right] - R\overline{T}\nabla^2\widetilde{q} && (11)\\
\frac{\partial \mathsf{d}}{\partial t} &= -\frac{g^2}{R\overline{T}}\tilde{\partial}(\tilde{\partial}+\mathcal{I})\mathcal{P} && (12)\\
\frac{\partial \widetilde{T}}{\partial t} &= -\frac{R\overline{T}}{C_v}(\nabla' u + \mathsf{d}) && (13)\\
\frac{\partial \mathcal{P}}{\partial t} &= \mathcal{S}\nabla' u - \frac{C_p}{C_v}(\nabla' u + \mathsf{d}) && (14)\\
\frac{\partial \widetilde{q}}{\partial t} &= -\mathcal{N}D + \frac{gs}{R\overline{T}}\mathcal{N}u && (15)
\end{aligned}$$

where the operator ∇' is defined by:

$$\nabla' = \nabla + \frac{s}{\overline{H}}\tilde{\partial} \tag{16}$$

and $\overline{H} = (R\overline{T}/g)$ (see Appendix A for other notations). The SI linear system $\mathcal{L}^*$ is obtained directly from the above system (11)–(15) by substituting $\overline{T} \to T^*$ and $s \to 0$

(and consequently $\nabla' \to \nabla$); it is of course not modified with respect to the case without orography. As a consequence, all terms associated to s are treated explicitly in (11)–(15). The method of analysis then follows the one proposed in B03, and the reader is invited to refer to this paper for the details of notations and the algebraic developments.

First, in this paragraph, the above system is shown to fulfil the four conditions [C1]–[C4] defined in B03, and which are required for making possible the space continuous analyses with the proposed method. The number of prognostic variables is $P = 4$ in the sense of B03, and the space continuous state-vector is $\mathcal{X} = (\mathcal{X}_1, \ldots, \mathcal{X}_4) = (D, \mathsf{d}, \widetilde{T}, \mathcal{P})$. The linear operator l in [C1] involves $l_1 = \tilde{\partial}$, $l_3 = \nabla$, and $l_4 = (\tilde{\partial} + \mathcal{I})\nabla$, respectively applied to (11), (13), and (14), as in section 7 of BLVS04. The "unbounded" linear system then becomes:

$$\tilde{\partial}\frac{\partial D}{\partial t} = R\overline{T}\nabla\nabla'\left[\frac{\widetilde{T}}{\overline{T}} - (\tilde{\partial} + \mathcal{I})\mathcal{P}\right] \tag{17}$$

$$\frac{\partial \mathsf{d}}{\partial t} = -\frac{g^2}{R\overline{T}}\tilde{\partial}(\tilde{\partial} + \mathcal{I})\mathcal{P} \tag{18}$$

$$\nabla\frac{\partial \widetilde{T}}{\partial t} = -\frac{R\overline{T}}{C_v}(\nabla' D + \nabla \mathsf{d}) \tag{19}$$

$$(\tilde{\partial} + \mathcal{I})\nabla\frac{\partial \mathcal{P}}{\partial t} = \nabla' D - \frac{C_p}{C_v}(\tilde{\partial} + \mathcal{I})(\nabla' D + \nabla \mathsf{d}) \tag{20}$$

The structure equation, which allows to determine the time-continuous normal modes of this linear system writes:

$$-\frac{1}{\overline{c}^2}\frac{\partial^4}{\partial t^4} + \frac{\partial^2}{\partial t^2}\left(\nabla'^2 + \frac{\tilde{\partial}(\tilde{\partial} + \mathcal{I})}{\overline{H}^2}\right) + \overline{N}^2\nabla'^2 = 0 \tag{21}$$

where:

$$\overline{c}^2 = \frac{C_p}{C_v}R\overline{T} \tag{22}$$

$$\overline{N}^2 = \frac{g^2}{C_p \overline{T}} \tag{23}$$

This structure equation appears to be formally similar to the structure equation without orography in BLVS04, except that the original horizontal gradient operator ∇ is replaced by ∇'. The determination of the continuous normal modes thus follows directly from the case without orography: the condition [C'2] requires $\overline{T} > 0$ and the structure of the normal modes of the continuous system is then given by:

$$\mathcal{X}_j(x,\sigma) = \widehat{\mathcal{X}_j} \exp\left[(ik_r + \frac{s}{2\overline{H}})x\right] \sigma^{(i\nu - 1/2)} \quad \text{for } j \in (1,\ldots,4) \tag{24}$$

where $\widehat{\mathcal{X}_j}$ is the complex magnitude for the considered variable, and $(k_r, \nu) \in \mathbb{R}$. Note that ν is a non-dimensional vertical wave-number, and $\nu = 2\pi$ represents a mode with a vertical wavelength equal to the characteristic height $\overline{H}$ of the atmosphere (here and in later similar uses related to waves geometry, π is of course 3.1415...). The real value π/k_r represents the horizontal half-wavelength of the mode, that is, the distance between two consecutive zeros of the real part of the complex mode along the x direction. For such a linear pertubation $\mathcal{X}_j(x,\sigma)$, the energy density of the perturbation is proportional to $\overline{\rho}\mathcal{X}_j^2$ where $\overline{\rho} = (\overline{\pi}/R\overline{T})$ (see e.g. Bannon, 1995). This energy density decomposes itself in three parts: kinetic, available potential, and available elastic energy density. The normal-modes (24) have an horizontal variation along constant σ surfaces which is consistent with the growth of the modes with height due to the Boussinesq effect and with the elevation of the terrain along the x axis. The normal modes $\mathcal{X}_j$ thus have a uniform amplitude along *true horizontal* surfaces only. However, the energy density of these normal modes is spatially uniform, as in the flat-terrain case, due to the compensating variation of the mass density $\overline{\rho}$:

$$\nabla(\overline{\rho}\mathcal{X}_j^2) = \tilde{\partial}(\overline{\rho}\mathcal{X}_j^2) = 0 \tag{25}$$

For an eigenmode characterized by (k_r, ν), the eigenvalues of derivative operators are:

$$\nabla = \left(ik_r + \frac{s}{2\overline{H}}\right) = ik \tag{26}$$

$$\tilde{\partial} = \left(i\nu - \frac{1}{2}\right) \tag{27}$$

$$\nabla' = i\left(k_r + \frac{s\nu}{\overline{H}}\right) = ik'. \tag{28}$$

The verification of [C3]–[C4] proceeds easily, as in the case without orography. It should be noted that for the reference system $l\mathcal{L}^*$, the ∇ operator is used everywhere, thus leading to the eigenvalue found in (26). For [C3], we have:

$$\xi_1 = (i\nu - 1/2) \tag{29}$$

$$\xi_3 = ik \tag{30}$$

$$\xi_4 = ik(i\nu + 1/2), \tag{31}$$

and for [C4]:

$$\overline{\mu}_{13} = -Rkk' \tag{32}$$

$$\mu_{13}^* = -Rk^2 \tag{33}$$

$$\overline{\mu}_{14} = R\overline{T}kk'(i\nu + 1/2) \tag{34}$$

$$\mu_{14}^* = RT^*k^2(i\nu + 1/2) \tag{35}$$

$$\overline{\mu}_{24} = \frac{g^2}{R\overline{T}}(\nu^2 + 1/4) \tag{36}$$

$$\mu_{24}^* = \frac{g^2}{RT^*}(\nu^2 + 1/4) \tag{37}$$

$$\overline{\mu}_{31} = -\frac{R\overline{T}}{C_v} ik' \tag{38}$$

$$\overline{\mu}_{32} = -\frac{R\overline{T}}{C_v} ik \tag{39}$$

$$\mu^*_{31} = \mu^*_{32} = -\frac{RT^*}{C_v} ik \tag{40}$$

$$\overline{\mu}_{41} = ik' \left[1 - \frac{C_p}{C_v}(i\nu + 1/2)\right] \tag{41}$$

$$\mu^*_{41} = ik \left[1 - \frac{C_p}{C_v}(i\nu + 1/2)\right] \tag{42}$$

$$\overline{\mu}_{42} = = \mu^*_{42} = -ik\frac{C_p}{C_v}(i\nu + 1/2). \tag{43}$$

All other μ_{ij} coefficients are zero, and [C1]–[C4] are finally fulfilled.

The analysis then proceeds as for the flat-terrain case in BLVS04: For the 3-TL SI scheme, a numerical growth-rate λ is introduced through:

$$\mathcal{X}(t) = \lambda \mathcal{X}(t - \Delta t) \tag{44}$$

$$\mathcal{X}(t + \Delta t) = \lambda^2 \mathcal{X}(t - \Delta t), \tag{45}$$

$$\tag{46}$$

and the stability equation can be expressed as in BLVS04:

$$\mathrm{Det}(\mathbf{M}) = 0, \tag{47}$$

where $\mathbf{M}$ is given by (46)–(49) of BLVS04, used with the above values of ξ_j and μ_{ij}. This eighth-degree stability polynomial equation in λ can be solved numerically: for any geometrical structure defined by a pair (k_r, ν), the modulus of the eight roots $\lambda_1(k_r, \nu), \ldots, \lambda_8(k_r, \nu)$ gives the growth rate of the eight corresponding eigenmodes. The growth-rate of the geometrical structure (k_r, ν) is then defined by the maximum modulus of the eight roots:

$$\Gamma(k_r, \nu) = \mathrm{Max}\left[\lambda_1(k_r, \nu), \ldots, \lambda_8(k_r, \nu)\right] \tag{48}$$

If one of the roots has a modulus larger than one, then the corresponding geometrical structure is unstable.

In this paper, the asymptotic growth-rate for a given geometrical structure (k_r, ν) is defined by the value of the above growth-rate in the limit of large time-steps. As discussed in B03, examination of asymptotic growth-rates is relevant since SI schemes are used with long time-steps in practice, and thus, asymptotic growth-rates provide a good indication of the robustness of a scheme independently of the particular value of the time-step.

For convenience, a parameter for the thermal nonlinearity can be introduced through

$$\alpha = \frac{\overline{T} - T^*}{T^*}. \tag{49}$$

As an illustration of the results, the asymptotic growth-rate for the kilometric scale horizontal mode with $k_r = 0.00157$ m^{-1} and for $\overline{T} = 280$ K is depicted in Fig. 1 as a function of α and s. The growth-rate which is plotted is the maximum growth-rate obtained when repeating the above analysis for discrete values of ν describing the interval [2 π, 100]. This interval represents vertical wavelenths varying between 500 m and $\overline{H}$. In practice however the maximum growth-rate for this figure is reached for the shortest vertical mode $\nu = 100$ (not shown). The domain where the growth-rate is smaller than 1.1 is restricted to a very small area along the axes, which means that for flows with significant values of the slope and the thermal nonlinearity, the scheme is highly unstable.

4 Stability analysis with the $\{\mathcal{P}, \mathbb{d}\}$ set of variables

As seen in BLVS04, the choice of the prognostic variables has a large impact on the stability of the SI EE system, and the presence of large nonlinear residuals in the elastic term D_3 is suspected to potentially lead to instabilities. In presence of orography, when d is used as prognostic variable, the elastic term D_3 actually has an explicitly treated thermal residual, given by the last RHS term of (8) in the linearized context. This residual, which is proportional to the slope, can thus be suspected to explain the instability found in the previous section when a slope is introduced. A new prognostic variable $\mathbb{d}$ which avoids this problem is examined here. In the general mass-based hybrid terrain following η coordinate of Laprise, 1992, this new variable $\mathbb{d}$ is defined by:

$$\mathbb{d} = \mathsf{d} + \frac{p}{mRT}\frac{\partial \mathbf{V}}{\partial \eta}.\boldsymbol{\nabla}\phi \tag{50}$$

where ϕ is the geopotential. In pure σ coordinate, and using $\mathcal{P}$ variable, this becomes:

$$\mathbb{d} = \mathsf{d} + \frac{(1+\mathcal{P})}{RT}\sigma\frac{\partial \mathbf{V}}{\partial \sigma}.\boldsymbol{\nabla}\phi \tag{51}$$

The elastic term D_3 writes in all cases:

$$D_3 = D + \mathbb{d} \tag{52}$$

The new variable $\mathbb{d}$ thus totally eliminates the thermal nonlinear residuals in the elastic term, even in presence of slanted coordinate surfaces.

The derivation of the linear system $\overline{\mathcal{L}}$ with the variable $\mathbb{d}$ is straightforward starting from (17)-(20). The geopotential gradient writes in σ coordinate:

$$\nabla\phi = \nabla\phi_s + R\int_\sigma^1 \nabla\left(\frac{T}{1+\mathcal{P}}\right)\frac{d\sigma'}{\sigma'} \tag{53}$$

which in the current linear context yields:

$$\nabla\phi = gs + R\overline{T}\mathcal{G}\nabla\left(\frac{\widetilde{T}}{\overline{T}} - \mathcal{P}\right) \tag{54}$$

The general relationship (50) between d and $\mathbb{d}$ thus becomes in the linear context:

$$\mathbb{d} = \mathsf{d} + \frac{gs}{R\overline{T}}\tilde{\partial}u \tag{55}$$

and the linear evolution equation for $\mathbb{d}$ writes:

$$\frac{\partial\mathbb{d}}{\partial t} = \frac{\partial\mathsf{d}}{\partial t} + \left(\frac{gs}{R\overline{T}}\tilde{\partial}\right)\frac{\partial u}{\partial t} \tag{56}$$

The original linearized system (11)-(14) for the d variable is thus modified into:

$$\begin{aligned}
\frac{\partial D}{\partial t} &= -R\overline{T}\nabla\nabla'\left[\mathcal{G}\frac{\widetilde{T}}{\overline{T}} - (\mathcal{G}-\mathcal{I})\mathcal{P}\right] - R\overline{T}\nabla^2\tilde{q} && (57)\\
\frac{\partial\mathbb{d}}{\partial t} &= -\frac{g^2}{R\overline{T}}\tilde{\partial}(\tilde{\partial}+\mathcal{I})\mathcal{P} + gs\nabla'\left[\frac{\widetilde{T}}{\overline{T}} - (\tilde{\partial}+\mathcal{I})\mathcal{P}\right] && (58)\\
\frac{\partial\widetilde{T}}{\partial t} &= -\frac{R\overline{T}}{C_v}(D+\mathbb{d}) && (59)\\
\frac{\partial\mathcal{P}}{\partial t} &= \mathcal{S}\nabla' u - \frac{C_p}{C_v}(D+\mathbb{d}) && (60)\\
\frac{\partial\tilde{q}}{\partial t} &= -\mathcal{N}D + \frac{gs}{R\overline{T}}\mathcal{N}u && (61)
\end{aligned}$$

Using the same operators l_1, l_3 and l_4 as previously, the linear system is then modified into the following "unbounded" version:

$$\begin{aligned}
\tilde{\partial}\frac{\partial D}{\partial t} &= R\overline{T}\nabla\nabla'\left[\frac{\widetilde{T}}{\overline{T}} - (\tilde{\partial}+\mathcal{I})\mathcal{P}\right] && (62)\\
\frac{\partial\mathbb{d}}{\partial t} &= -\frac{g^2}{R\overline{T}}\tilde{\partial}(\tilde{\partial}+1)\mathcal{P} + gs\nabla'\left[\frac{\widetilde{T}}{\overline{T}} - (\tilde{\partial}+\mathcal{I})\mathcal{P}\right] && (63)\\
\nabla\frac{\partial\widetilde{T}}{\partial t} &= -\frac{R\overline{T}}{C_v}(\nabla D + \nabla\mathbb{d}) && (64)
\end{aligned}$$

$$(\tilde{\partial}+\mathcal{I})\nabla\frac{\partial\mathcal{P}}{\partial t} = \nabla' D - \frac{C_p}{C_v}(\tilde{\partial}+\mathcal{I})(\nabla D + \nabla \mathbf{d}) \tag{65}$$

The structure equation is still given by (21), the structure of normal modes by (24), and the eigenvalues of spatial operators by (26)–(28). The ξ_i coefficients are unchanged, and the μ_{ij} coefficients which are modified with respect to the previous analysis with d are:

$$\overline{\mu}_{23} = \frac{gs}{\overline{T}}ik' \tag{66}$$

$$\overline{\mu}_{24} = \frac{g^2}{R\overline{T}}(\nu^2+1/4) - gsik'(i\nu+1/2) \tag{67}$$

$$\overline{\mu}_{31} = -\frac{R\overline{T}}{C_v}ik \tag{68}$$

$$\overline{\mu}_{41} = ik' - \frac{C_p}{C_v}ik(i\nu+1/2) \tag{69}$$

These new coefficients are used to build the new matrix $\mathbf{M}$ and the analysis proceeds similarly to the previous case, by solving (47).

Figure 2 shows the asymptotic growth-rate in the same conditions as for Fig. 1 but for the new variable $\mathbb{d}$ instead of the variable d (it is worth noticing that the figure has no reason to be symmetric around the $s = 0$ axis since the stability may depend on the relative value of the coordinate slope and of the wave-surfaces slope). The domain for which the growth-rate is smaller than 1.1 is now much larger than in Fig. 1, clearly indicating an enhanced robustness of the scheme with the new prognostic variable $\mathbb{d}$ for this structure. In opposition with the d variable, the maximum growth-rate depicted on the figure is not always obtained for the shortest vertical mode: for instance the unstable areas located near $s = \pm 0.05$ and $\alpha \approx \mp 0.2$ are not due to the shortest vertical mode (not shown).

However, even if using the new variable $\mathbb{d}$ globally enhances the stability, it does not guarantee a formal stability of the scheme for arbitrarily long time-steps in the context of the analysis. As indicated by the shape of the contour line $\Gamma = 1.01$ in Fig. 2, the scheme

is in fact formally stable only for $s = 0$ and $\alpha \in [-0.5, 1]$. As soon as $s \neq 0$, the $\mathbb{d}$ variable still leads to a formal instability (although much weaker than for the d variable). This behaviour contrasts with the formal stability obtained with d for flat terrains in BLVS04, even in the long time-steps limit. The analyses presented above thus indicate that when orography is present, the EE system is not likely to be solved in a stable way with a SI scheme using arbitrarily long time-steps even with the $\mathbb{d}$ variable.

The stability of the same horizontal mode $k_r = 0.00157$ as in the previous figures is now examined when the time-step is reduced to $\Delta t = 100$ s. This time-step represents a realistic (although ambitious) value for a model which would resolve the considered mode k_r with a 3-TL SI time-discretization. Figure 3 shows the growth-rate obtained for this time-step with the d variable (note the modified shading limits compared to Figs. 1 and 2). Not surprisingly, the growth-rate decreases when the time-step is reduced, however, the values of the growth-rate when s and α significantly deviate from 0 are still incompatible with a practical use. The growth-rate obtained in the same conditions with the variable $\mathbb{d}$ is depicted in Fig. 4. Here also, a formal stability is obtained only for $s = 0$ as indicated by the shape of the contour line $\Gamma = 1.001$, however, the value of the growth-rate is very close to 1 in a wide area (in practice α has a typical absolute magnitude smaller than 0.2), and the scheme can be considered as viable when used in a space-discretized model, in which many processes are likely to act in a diffusive fashion.

5 Numerical assessment in the academic context

In order to demonstrate the qualitative relevance of the previous analyses, a similar academic context is reproduced in the spectral Aladin-NH numerical model documented in BHBG95. A non-rotating adiabatic vertical-plane version of the model is used, with a

resting, isothermal and hydrostatically-balanced initial state.

The horizontal domain is horizontally cyclic, 64 km wide with a 21 spectral truncation, thus allowing a minimum horizontal wavelength of about 3048 m. The vertical domain consists in 60 regularly spaced σ levels. The value of the time-step is $\Delta t = 50$ s.

For practical reasons, the orography does not consist of a constant slope as in the analyses but is taken as a cosine function of same wavelength as the horizontal width of the domain. The deviation of the cosine orography is $\pm$ 500 m, thus resulting in two areas of opposed maximum slope $s = \pm 0.05$.

The model is made free of any damping process (horizontal diffusion, SI time-filter,...), however, a weak classical Asselin time-filter ($\epsilon = 0.01$) is applied to prevent a separation of physical and computational modes resulting from the leap-frog time-discretization. A very small random initial wind perturbation is introduced in order to prevent an undeterministic evolution when the initial equilibrium state is physically stable but numerically unstable. The atmospheric and reference temperature are set to 285 K and 350 K respectively (hence $\alpha \approx$ -0.186).

The experiment with d numerically diverges after 49 time-steps: an unstable flow develops above the areas of maximum slope. For the experiments with $\mathbf{d}$, the integration remains stable after 2000 time-steps: the discretization processes acting in a numerical model (including semi-Lagrangian interpolations) are able to stabilize unstable modes when their growth-rate is very small. However, the instability for large time-steps appears when Δt is pushed to 200 s: the experiment with d and $\mathbb{d}$ respectively diverges after 10 and 41 time-steps, qualitatively confirming the results of the previous analyses.

6 Comments

Since no stability analysis of constant-coefficients SI schemes with orography and NL thermal residuals has been reported in the earlier literature, it is interesting to examine what is the situation for the HPE system. A similar (although more simple) analysis can be performed for the HPE system. In this case, the $\overline{\mathcal{L}}$ system reduces to:

$$\frac{\partial D}{\partial t} = -R\nabla\nabla'\mathcal{G}\widetilde{T} - R\overline{T}\nabla^2\widetilde{q} \tag{70}$$

$$\frac{\partial \widetilde{T}}{\partial t} = -\frac{R\overline{T}}{C_p}\mathcal{S}\nabla' u \tag{71}$$

$$\frac{\partial \widetilde{q}}{\partial t} = -\mathcal{N}D + \frac{gs}{R\overline{T}}\mathcal{N}u. \tag{72}$$

Following the formalism of B03, a linear vertical operator $\left[l_1 = \tilde{\partial}, l_2 = (\tilde{\partial} + \mathcal{I})\nabla\right]$ can be applied to the previous system: the number of prognostic variables for the unbounded system is then $P = 2$, the state variable is $(D, \widetilde{T})$. For the [C3] condition, we have:

$$\xi_1 = (i\nu - 1/2) \tag{73}$$

$$\xi_2 = ik(i\nu + 1/2), \tag{74}$$

and for [C4]:

$$\overline{\mu}_{12} = -Rkk' \tag{75}$$

$$\mu^*_{12} = -Rk^2 \tag{76}$$

$$\overline{\mu}_{21} = -\frac{R\overline{T}}{C_p}ik' \tag{77}$$

$$\mu^*_{21} = -\frac{RT^*}{C_p}ik \tag{78}$$

$$\tag{79}$$

All other μ_{ij} coefficients are zero. The analysis then follows as in previous sections. The growth-rate for $\Delta t = 100$ s and $k_r = 0.00157$ as in Figs. 3 and 4 is depicted in Fig. 5 for the HPE system. A weak instability is present in the considered domain with a magnitude roughly similar to the one obtained with the $\mathbb{d}$ variable. Hence the weak instability of the SI scheme in presence of orography found with $\mathbb{d}$ is not a new feature of the EE system, but was already present in the HPE system, although not reported in the earlier literature. This may be explained by the fact that this instability is maybe too weak to significantly endanger current practical NWP applications.

It should be noted that the dramatic sensitivity to the choice of the prognostic variables with sloped-terrain, as discussed in sections 3, 4, also exists for EE systems in height-based coordinates with constant-coefficients SI schemes, such as e.g. in the CRCM model (Caya and Laprise, 1999, CL99 hereafter): as discussed in BLVS04, the natural choice for the vertical momentum variable for these models would be the vertical velocity w, but this choice was experimentally found to result in a very unstable SI scheme with sloped terrain (Laprise, personal communication). To solve this problem, these models use, as a prognostic variable, the contravariant vertical velocity W [given by (21) of CL99], which, in the context of height-based coordinated is the counterpart of $\mathbb{d}$ in mass-based coordinates.

7 Alternative time treatment for the cross-term of $\mathbb{d}$

The use of $\mathbb{d}$ in mass-based coordinates, as well as W in height-based coordinates (when a constant-coefficients approach is used as in CL99), leads to a practical problem for the complete (nonlinear) system, since these prognostic variables have rather cumbersome evolution equations. Considering (50), the evolution equation for $\mathbb{d}$ would involve a very

large number of terms coming from the evolution of the so-called cross-term, that is, the last term in the right hand side (rhs) of (50). Similar complications occur for W in height-based Gal-Chen coordinates.

The solution adopted to circumvent this problem is illustrated here for the $\mathbb{d}$ variable in the general hybrid mass-based coordinate η, but a similar argument can be developped for W in height based coordinates. The $\mathbb{d}$ equation is written as follows:

$$\frac{d\mathbb{d}}{dt} = RHS\left(\frac{d\mathsf{d}}{dt}\right) + \frac{d}{dt}\left(\frac{p}{mRT}\frac{\partial \mathbf{V}}{\partial \eta}.\boldsymbol{\nabla}\phi\right), \tag{80}$$

where $RHS\,(d\mathsf{d}/dt)$ is the rhs of the complete (nonlinear) evolution equation for d. This latter rhs is much simpler than the total rhs of (80), and is treated in the classical SI fashion: it is separated into a linear part $\mathcal{L}^*_{\mathsf{d}}(\mathcal{X})$ and a non-linear residual $\mathcal{M}_{\mathsf{d}}(\mathcal{X}) - \mathcal{L}^*_{\mathsf{d}}(\mathcal{X})$ exactly as for the d equation. Since the coefficients μ^*_{ij} are identical in sections 3 and 4, the linear part $\mathcal{L}^*_{\mathbb{d}}(\mathcal{X})$ of the $\mathbb{d}$ evolution equation is equal to $\mathcal{L}^*_{\mathsf{d}}(\mathcal{X})$. Then the evolution equation for $\mathbb{d}$ is time-discretized as:

$$\begin{aligned}\frac{\mathbb{d}^+ - \mathbb{d}^-}{2\Delta t} &= \mathcal{M}_{\mathsf{d}}(\mathcal{X}^0) - \mathcal{L}^*_{\mathsf{d}}(\mathcal{X}^0) + \frac{\mathcal{L}^*_{\mathsf{d}}(\mathcal{X}^+) + \mathcal{L}^*_{\mathsf{d}}(\mathcal{X}^-)}{2} \\ &+ \frac{1}{\Delta t}\left[\left(\frac{p}{mRT}\frac{\partial \mathbf{V}}{\partial \eta}.\boldsymbol{\nabla}\phi\right)^0 - \left(\frac{p}{mRT}\frac{\partial \mathbf{V}}{\partial \eta}.\boldsymbol{\nabla}\phi\right)^-\right]\end{aligned} \tag{81}$$

where superscripts $-$, $+$, and 0 represent variables at time $(t - \Delta t)$, $(t + \Delta t)$ and t respectively. Hence, the linear part of the $\mathbb{d}$ equation has a centred implicit treatment, the $(\mathcal{M}_{\mathsf{d}} - \mathcal{L}^*_{\mathsf{d}})$ part is treated explicitely, and the last term of (80) is treated in a diagnostic way from the two most recent available states.

The same approach is applied in models with height-based vertical coordinates and constant-coefficients SI schemes, in order to avoid the cumbersome evolution equation of W. For instance in CL99, the combination of their Eqs. (48) and (52) leads to a single

prognostic equation for W formally similar to the above equation (81).

The stability analysis for the SI scheme with the $\mathbf{d}$ variable presented in section 4 can be easily adapted to take into account the specific time-treatment of the $\mathbf{d}$ equation. A $l_2 = \nabla$ operator is applied to (56) in order to eliminate u in favour of D in the last term. Hence for the [C3] condition:

$$\xi_2 = ik \tag{82}$$

and two $\overline{\mu}_{ij}$ coefficients must be modified with respect to section 4:

$$\overline{\mu}_{23} = 0 \tag{83}$$

$$\overline{\mu}_{24} = \frac{g^2}{R\overline{T}} ik(\nu^2 + 1/4). \tag{84}$$

A new set of coefficients $\overline{\overline{\mu}}_{ij}$ must be introduced:

$$\overline{\overline{\mu}}_{21} = \frac{gs}{R\overline{T}}(i\nu - 1/2), \tag{85}$$

all other $\overline{\overline{\mu}}_{ij}$ coefficients being equal to zero. Finally, the matrix M_1 in Eq. (47) of BLVS04 must be modified to:

$$(M_1)_{ij} = -\delta_{ij} - \Delta t \frac{\overline{\mu}_{ij}}{\xi_i} - 2(\lambda - 1)\frac{\overline{\overline{\mu}}_{ij}}{\xi_i} \tag{86}$$

For $\Delta t = 100$ s, the results for the stability are not significantly modified with respect to those obtained with the normal treatment of $\mathbf{d}$ as seen in Fig. 6. For long time-steps, this time treatment brings a further increase of stability compared to the normal treatment (not shown).

These specific time treatments with $\mathbf{d}$ and W variables thus combine the advantages of an increased simplicity and a similar robustness. Their main disadvantage is that they are

only first-order accurate in time. The generally accepted requirement that NWP models should be globally second-order accurate in time is thus violated for the terms treated in this way. However, the impact of these treatments can be easily evaluated in a given model by changing the size of the time-step, and no particular problem linked to this point has been reported so far (e.g. in the CRCM model). Moreover, it should be noted that this disdvantage disappears by construction for iterative centered implicit (ICI) schemes as defined in B03. These ICI schemes, based on a larger number of iterations of the linear implicit equation inversion, have been shown in B03 to be more robust than the SI scheme, and could be an interesting alternative for the fully compressible meso-scale NWP in the future, especially when the the physical parameterizations are costly compared to the dynamical kernel of the considered model.

8 Conclusion

The stability of constant-coefficients 3-TL SI schemes for the EE and HPE systems has been examined in the case of a uniform slope orography in presence of explicit thermal residuals. It has been shown that for the EE system, the presence of this slope reduces furthermore the set of the prognostic variables which can be used for the vertical momentum equation. The only possible variables are those for which the elastic term D_3 has no nonlinear residual in presence of slope. The variable proposed in the mass-coordinate context of this paper obviously meets this criterion, since it writes $\mathbb{d} = D_3 - D$, and D is also a prognostic variable. The resulting robustness has been shown to be similar to the one observed for the HPE system in presence of slope. For prognostic variables such as $\mathbb{d}$ (in mass-based coordinates) or W (in height-based coordinates), the evolution equation is cumbersome, and an alternative time-treatment of some terms is required. However,

further analyses have shown that this treatment does not modify significantly the stability of the SI scheme.

This paper, together with B03, BLVS04 and B04 forms a complete set which allows to better understand the behaviour of the EE system with constant-coefficients SI (or ICI) time-schemes from the theoretical point of view. The general learning drawn from this set of papers is that provided a great care is taken about all the details of the formulation, the robustness of the EE system with constant-coefficients SI schemes should be comparable to the one of the HPE system, and compatible with meso-scale NWP purposes.

The modifications proposed in this series of papers have been implemented in the Aladin-NH model (including the possibility of using ICI schemes), resulting in what may finally be viewed as a new dynamical kernel for this model.

Another general learning is that there is a deep formal dualism between the systems cast in height-based and mass-based coordinates as far as constant-coefficient SI schemes are concerned. Except the fact that the specification of a reference pressure profile is mandatory in height-based systems with constant-coefficients SI schemes, a feature which has no equivalent in mass-based systems, no significant difference was found between the two classes of systems in terms of behaviour and stability. Another illustration of this dualism can be found in the very simple form that takes the relaxation of the shallow-atmosphere approximation in the mass-based EE system (Wood and Staniforth, 2003) similarly to height-based systems. We claim that this dualism invalidates a common (though not published) belief according to which height-based coordinates are the best suited ones to build efficients nonhydrostatic models.

Finally, it should be noted that the constant-coefficients schemes examined here, when coupled with iterative (ICI) schemes represent an alternative approach to schemes with non-constant coefficients as proposed by Skamarock et al. (1997) or Thomas et al. (1998).

Together with Côté et al. (1998) and Cullen (2001), we believe this approach is worth being considered for solving the EE system in a stable and accurate manner.

Acknowledgments: Part of the research reported in this paper was supported by the ALATNET grant HPRN-CT-1999-00057 of the European Union TMR/IHP Programme. We gratefully acknowledge helpful discussions with Jozef Vivoda.

Appendix A : List of Symbols

vertical spatial operators in σ coordinate:

$\mathcal{G}X = \int_\sigma^1 (X/\sigma')d\sigma'$

$\mathcal{S}X = (1/\sigma)\int_0^\sigma Xd\sigma'$

$\mathcal{N}X = \int_0^1 Xd\sigma$

$\mathcal{I}X = X$

$\tilde{\partial}X = \sigma(\partial X/\partial\sigma)$

miscellaneous symbols:

∇ : $(\partial/\partial x)$ along constant levels of the considered vertical coordinate.

$\boldsymbol{\nabla}$: vector horizontal gradient operator along constant levels of the considered vertical coordinate.

$(\partial/\partial t)$: Eulerian time derivative

(d/dt) : Lagrangian time-derivative

g : gravitational acceleration

R, C_p, C_v : dry air thermodynamic constants

π_s : hydrostatic surface-pressure (proportional to the column-integrated mass in a Cartesian system as outlined in Wood and Staniforth, 2003).

References

Bannon, P. R., 1995: Hydrostatic adjustment; Lamb's problem. *J. Atmos. Sci*, **52**, 1743–1752.

Bénard, P., 2003: Stability of semi-implicit and iterative centered-implicit time discretizations for various equation systems used in NWP. *Mon. Wea. Rev.*, **131**, 2479-2491.

Bénard, P., 2004: On the use of a wider class of linear systems for the design of constant-coefficients semi-implicit time-schemes in NWP. *Mon. Wea. Rev.*, **132**, 1319-1324.

Bénard, P., R. Laprise, J. Vivoda and P. Smolíková, 2004: Stability of the leap-frog constant-coefficients semi-implicit scheme for the fully elastic system of Euler equations. Flat terrain case. *Mon. Wea. Rev.*, **132**, 1306-1318.

Bubnová, R., G. Hello, P. Bénard, and J.F. Geleyn, 1995: Integration of the fully elastic equations cast in the hydrostatic pressure terrain-following coordinate in the framework of the ARPEGE/Aladin NWP system. *Mon. Wea. Rev.*, **123**, 515-535.

Caya, D., and R. Laprise, 1999: A semi-implicit semi-Lagrangian regional climate model: the Canadian RCM. *Mon. Wea. Rev.*, **127**, 341-362.

Côté, J., M. Béland, and A. Staniforth, 1983: Stability of vertical discretization schemes for semi-implicit primitive equation models: theory and application. *Mon. Wea. Rev.*, **111**, 1189-1207.

Côté, J., S. Gravel, A. Méthot, A. Patoine, M. Roch, and A. Staniforth, 1998: The Operational CMC-MRB Global Environmental Multiscale (GEM) Model. Part I: Design Considerations and Formulation. *Mon. Wea. Rev.*, **126**, 1373-1395.

Ikawa, M., 1988: Comparison of some schemes for nonhydrostatic models with orography. *J. Meteorol. Soc. Jpn.*, **66**, 753-776.

Laprise, R., 1992: The Euler equations of motion with hydrostatic pressure as an independent variable. *Mon. Wea. Rev.*, **120**, 197-207.

Qian, J.-H., F. H. M. Semazzi, and J. S. Scroggs, 1998: A global nonhydrostatic semi-Lagrangian atmospheric model with orography. *Mon. Wea. Rev.*, **126**, 747-771.

Robert, A. J., J. Henderson, and C. Turnbull, 1972: An implicit time integration scheme for baroclinic models of the atmosphere . *Mon. Wea. Rev.*, **100**, 329-335.

Simmons, A. J., C. Temperton, 1997: Stability of a two-time-level semi-implicit integration scheme for gravity wave motion. *Mon. Wea. Rev.*, **125**, 600-615.

Simmons, A. J., B. Hoskins, and D. Burridge, 1978: Stability of the semi-implicit method of time integration. *Mon. Wea. Rev.*, **106**, 405-412.

Skamarock, W. C., P. K. Smolarkiewicz, and J. B. Klemp, 1997: Preconditioned conjugate-residual solvers for Helmholtz equations in nonhydrostatic models. *Mon. Wea. Rev.*, **125**, 587-599.

Wood, N. and A. Staniforth, 2003: The deep-atmosphere Euler equations with a mass-based vertical coordinate. *Quart. J. Roy. Meteor. Soc.*, **129**, 1289-1300.

Thomas, S.J., C. Girard, R. Benoit, M. Desgagné, and P. Pellerin, 1998: A new adiabatic kernel for the MC2 model. *Atmos. Ocean*, **36 (3)**, 241-270.

List of Figures

Fig. 1: Growth-rate for the simplified problem as a function of the nonlinearity parameter α and slope s for the variable d with $\Delta t = +\infty$.

Fig. 2: Growth-rate for the simplified problem as a function of the nonlinearity parameter α and slope s for the variable $\mathbb{d}$ with $\Delta t = +\infty$.

Fig. 3: Growth-rate for the simplified problem as a function of the nonlinearity parameter α and slope s for the variable d with $\Delta t = 100$ s.

Fig. 4: Growth-rate for the simplified problem as a function of the nonlinearity parameter α and slope s for the variable $\mathbb{d}$ with $\Delta t = 100$ s.

Fig. 5: Growth-rate for the simplified problem as a function of the nonlinearity parameter α and slope s for the HPE system with $\Delta t = 100$ s.

Fig. 6: Growth-rate for the simplified problem as a function of the nonlinearity parameter α and slope s for the $\mathbb{d}$ variable with the alternative time-treatment, and with $\Delta t = 100$ s.

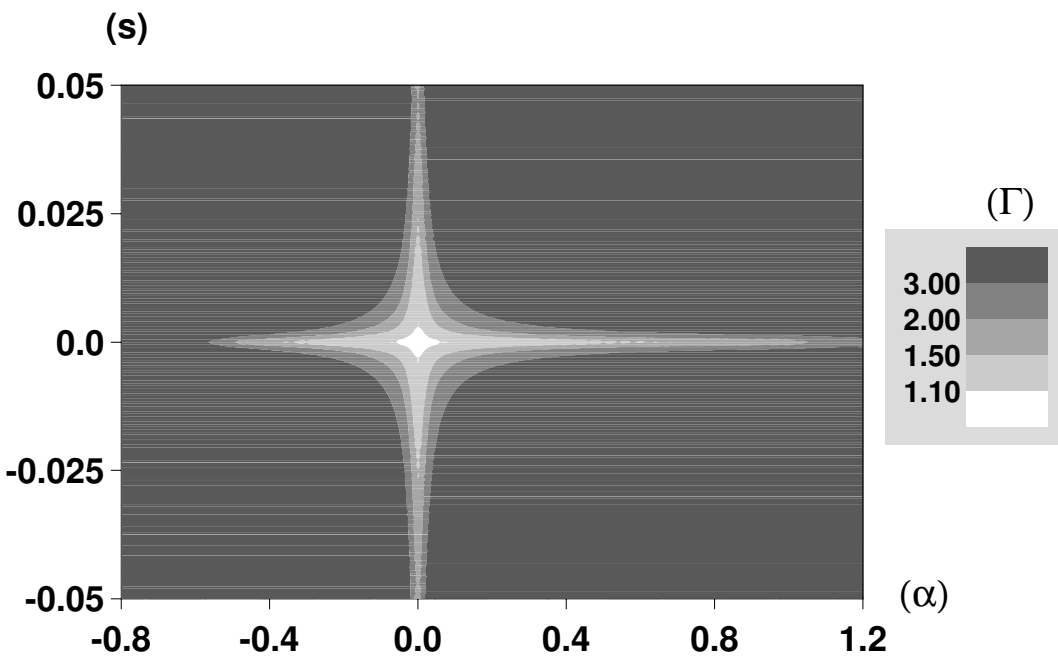

Figure 1: Growth-rate for the simplified problem as a function of the nonlinearity parameter α and slope s for the variable d with $\Delta t = +\infty$.

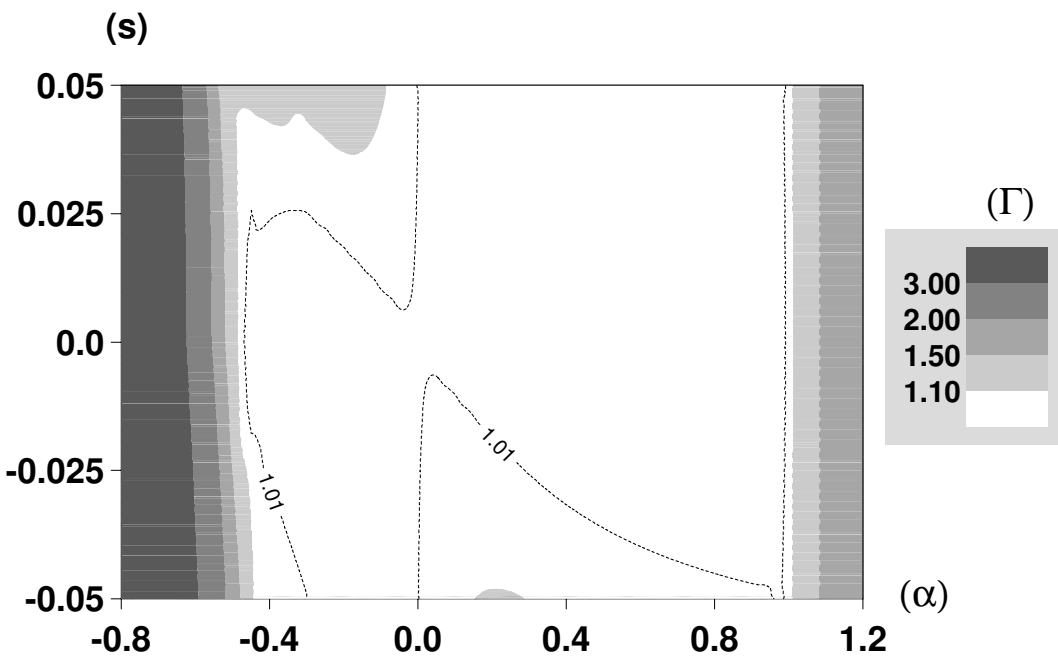

Figure 2: Growth-rate for the simplified problem as a function of the nonlinearity parameter α and slope s for the variable $\mathbb{d}$ with $\Delta t = +\infty$.

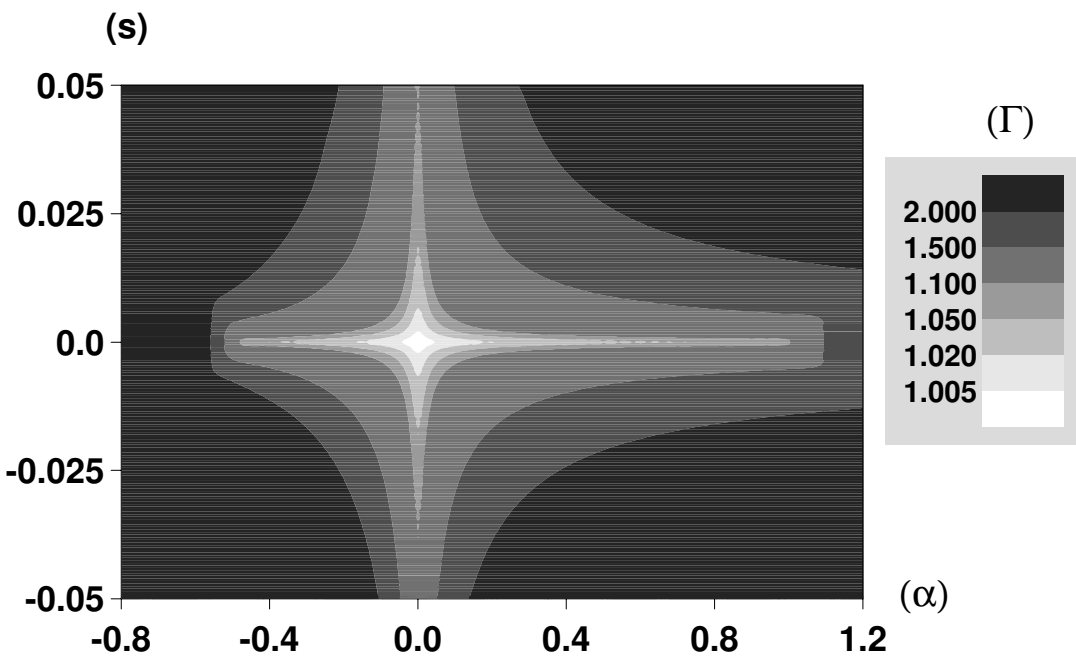

Figure 3: Growth-rate for the simplified problem as a function of the nonlinearity parameter α and slope s for the variable d with $\Delta t = 100$ s.

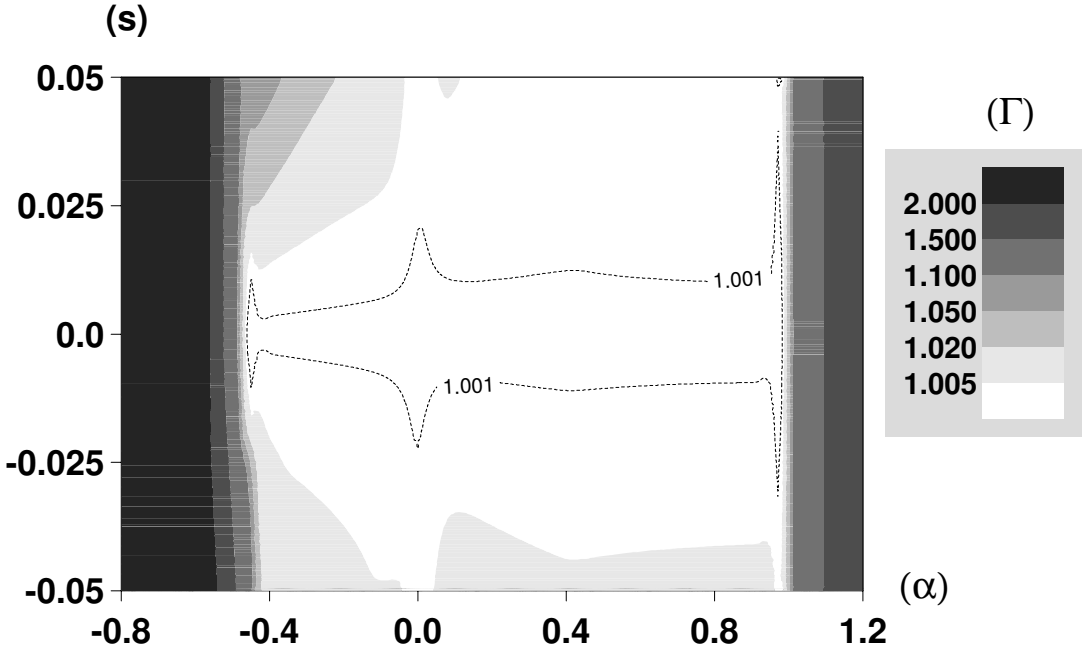

Figure 4: Growth-rate for the simplified problem as a function of the nonlinearity parameter α and slope s for the variable dl with $\Delta t = 100$ s.

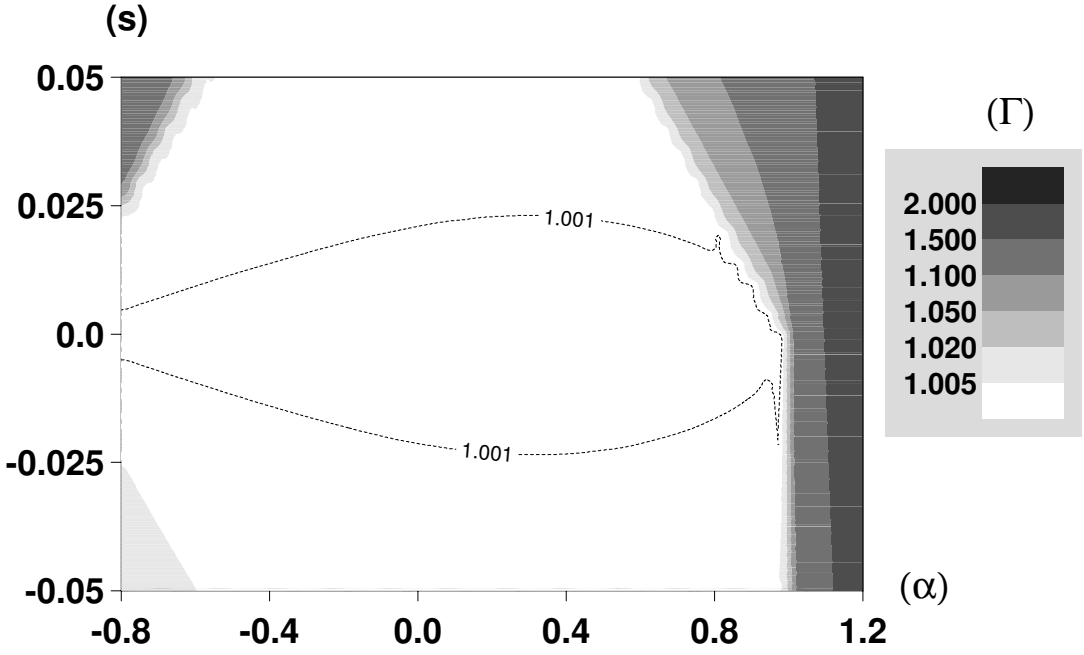

Figure 5: Growth-rate for the simplified problem as a function of the nonlinearity parameter α and slope s for the HPE system with $\Delta t = 100$ s.

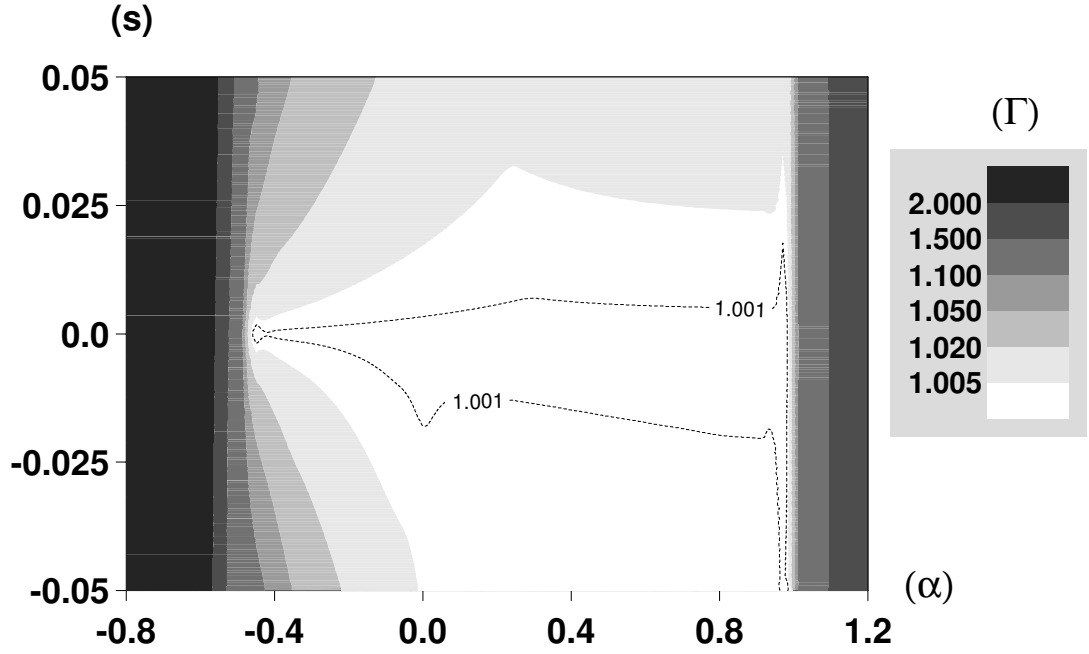

Figure 6: Growth-rate for the simplified problem as a function of the nonlinearity parameter α and slope s for the dl variable with the alternative time-treatment, and with $\Delta t = 100$ s.